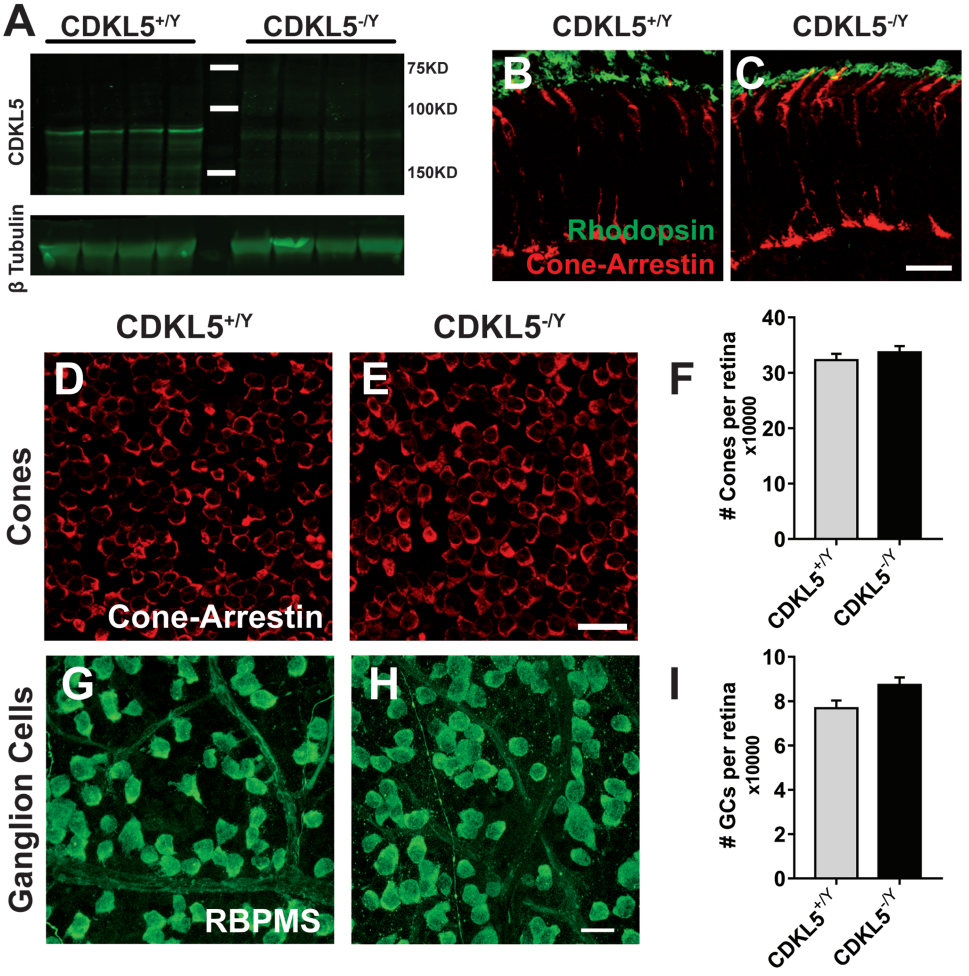

Figure 1. CDKL5 null mice show normal retinal morphology. **(A)** Western blot analysis on adult male CDKL5$^{-/y}$ and WT (CDKL5$^{+/y}$) retinal homogenates showing CDKL5 expression. **(B and C)** Retinal sections stained for cone photoreceptors (cone arrestin, red) and rod outer segments (rhodopsin, green). The overall structural organization of photoreceptor cells is identical in the two experimental groups. **(D and E)** Representative images from retinal whole-mount preparations of CDKL5$^{+/y}$ (D) and CDKL5$^{-/y}$ (E) stained for cone arrestin as a cone marker. **(F)** Quantitation of the total number of cones showed no statistical significance between the two groups (two-tailed Student's *t*-test $P = 0.435$). **(G and H)** Representative images from retinal whole-mount preparations of CDKL5$^{+/y}$ (G) and CDKL5$^{-/y}$ (H) stained for RBPMS as a RGCs marker. **(I)** Quantitation of the total number of cones (I) showed no statistical significance between the two groups (two-tailed Student's *t*-test $P = 0.098$). Scale bars are equal to 20 μm. Error bars represent standard error of mean (SEM).

(Fig. 2B; two-tailed Student's *t*-test $P = 0.026$). To evaluate spine morphology, we classified spines as immature (filopodia, thin-shaped and stubby-shaped) or mature (mushroom and cup-shaped) (20,39). CDKL5 null mice had a greater proportion of immature spines (Fig. 2C; χ^2 test $P = 0.0027$) compared to the controls. Furthermore, the distribution of spines in classes was significantly skewed toward a more immature state in mice lacking CDKL5 (Fig. 2D; χ^2 test $P = 0.0009$). To corroborate this result we performed immunohistochemistry (IHC), staining for PSD95, a postsynaptic marker of excitatory synapse maturation (32). Consistently with Golgi-staining data, CDKL5$^{-/y}$ mice ($N = 6$) showed a strong decrease in the density of PSD95 positive puncta with respect to CDKL5$^{+/y}$ ($N = 6$; two-tailed Student's *t*-test $P < 0.0001$; Fig. 2E and F). Moreover, to assess the impact of the lack of CDKL5 onto inhibitory circuitry, we stained for VGAT, a presynaptic marker of inhibitory synapses (5). The results showed no significant alterations in VGAT positive puncta suggesting that the lack of CDKL5 produces synaptic alterations in the dLGN occurring at the level of excitatory connections.

Previous *in vivo* studies (8) showed that CDKL5 knockout mice demonstrated decreased dendritic spine stability in cortical neurons in the somatosensory cortex. We, therefore, asked whether a spine density deficit was present in V1. This possibility was suggested by findings showing downregulation of the density of PSD95 positive puncta in this area (27). Golgi-staining in V1 coronal slices of CDKL5 KO mice unveiled a decreased spine density in layer 2/3 (Fig. 3) and layer 5 (Supplementary Material, Fig. S3) apical dendrites of pyramidal neurons in CDKL5$^{-/y}$ animals ($N = 4$) with respect to CDKL5$^{+/y}$ controls (Fig. 3A; $N = 5$; two-tailed Student's *t*-test $P < 0.003$; Supplementary Material, Fig. S3A). Furthermore, analyzing the distribution of spines in morphological classes, we found a lower proportion of mature spines (Fig. 3B; Fisher's exact test $P < 0.001$; Supplementary Material, Fig. S3B) and an increased fraction of filopodia-like, thin and stubby spines (Fig. 3C; χ^2 test $P < 0.001$; Supplementary Material, Fig. S3C). These morphological abnormalities were coupled to a reduction in the PSD95$^+$ puncta in CDKL5$^{-/y}$ ($N = 6$) versus CDKL5$^{+/y}$ (Fig. 3D and E; $N = 6$; two-tailed Student's *t*-test $P < 0.001$) animals, confirming previous